Research Article

Muhammad Nasir Amin*, Faizullah Jan, Kaffayatullah Khan*, Suleman Ayub Khan*, Muhammad Tahir Qadir, and Marcin Kujawa

Tensile behavior evaluation of two-stage concrete using an innovative model optimization approach

https://doi.org/10.1515/rams-2025-0097
received June 28, 2024; accepted February 17, 2025

Abstract: Two-stage concrete (TSC) is a sustainable material produced by incorporating coarse aggregates into formwork and filling the voids with a specially formulated grout mix. The significance of this study is to improve the predictive accuracy of TSC's tensile strength, which is essential for optimizing its use in construction applications. To achieve this objective, novel and reliable predictive models were developed using advanced machine learning algorithms, including random forest (RF) and gene expression programming (GEP). The performance of these models was evaluated using important evaluation metrics, including the coefficient of determination (R^2), mean absolute error (MAE), mean squared error, and root mean square error (RMSE), after they were trained on a comprehensive dataset. The results suggest that the RF model outperforms the GEP model, as evidenced by a higher R^2 value of 0.94 relative to 0.91 for GEP and reduced MAE and RMSE error values. This suggests that the RF model has a superior predictive capability. Additionally, sensitivity analyses and SHapley Additive ExPlanation analysis revealed that the water-to-binder (W/B) ratio was the most influential input parameter, accounting for 51.01% of the predictive outcomes presented in the model. This research emphasizes optimizing TSC design, enhancing material performance, and promoting sustainable, cost-effective construction.

Keywords: two-stage concrete, tensile strength, machine learning

1 Introduction

Two-stage concrete (TSC) is a specialized type of concrete that is produced using a process that is distinct from conventional concrete. The initial step in TSC entails the stuffing of the formwork with coarse aggregate particles. Subsequently, a highly fluid grout mixture is employed to occupy the cavities between the particles of aggregate. The fundamental structural component of TSC is the coarse aggregate, which comprises approximately 60% of the material [1]. By directing stresses onto the aggregate particles' points of contact, TSC achieves an exceptionally accurate stress distribution [2]. These forces may cause aggregate particles to shatter or separate from grout [3]. The grout used in TSC is composed of water, well-graded sand, chemical admixtures, and ordinary Portland cement (OPC). In certain TSC formulations, blended binders are now included as a result of the presence of supplementary cementitious materials (SCMs). The flowability of grout, water requirements, and heat generated during hydration can all be enhanced by replacing approximately 33% of OPC with fly ash [4,5]. Despite its unique characteristics and potential advantages in construction, the existing body of research on TSC remains limited. Many studies focus on traditional concrete, with comparatively fewer investigations exploring TSC's mechanical behavior and durability. As the demand for sustainable and high-performance concrete solutions grows, understanding TSC's properties becomes increasingly important. However, the time-consuming and costly nature of experimental evaluations has hindered extensive research in this area.

It is anticipated that the utilization of TSC will experience a substantial increase in the years ahead due to the

* **Corresponding author: Muhammad Nasir Amin,** Department of Civil and Environmental Engineering, College of Engineering, King Faisal University, Al-Ahsa, 31982, Saudi Arabia, e-mail: mgadir@kfu.edu.sa
* **Corresponding author: Kaffayatullah Khan,** Department of Civil and Environmental Engineering, College of Engineering, King Faisal University, Al-Ahsa, 31982, Saudi Arabia, e-mail: kkhan@kfu.edu.sa
* **Corresponding author: Suleman Ayub Khan,** Department of Civil Engineering, COMSATS University Islamabad, Abbottabad, 22060, Pakistan, e-mail: sulemanayub@cuiatd.edu.pk
Faizullah Jan, Marcin Kujawa: Faculty of Civil and Environmental Engineering, Gdańsk University of Technology, Gdańsk, Poland
Muhammad Tahir Qadir: Department of Civil and Environmental Engineering, College of Engineering, King Faisal University, Al-Ahsa, 31982, Saudi Arabia

ongoing expansion of concrete in construction projects. However, despite the multiple benefits that TSCs provide, only a small number of study examinations have been conducted on them. It was determined that the highest quality mortar is produced by a cement–sand ratio of 1 and a water-to-cement ratio of 0.47 when developing TSC [6]. Furthermore, the incorporation of silica fume (SF) as a partial replacement for OPC exhibits two opposing impacts on the properties of the TSC: it simultaneously improves the strength of the TSC while diminishing the workability of the grout [2]. The workability of TSC grouts is decreased as a result of the incorporation of SF as a micro-filler that is designed to fill the crevices between the particles of sand and cement during the preparation process [2]. This is because SF has a very large surface area, which increases the water demand. Simultaneously, SF undergoes a vigorous reaction with CH, resulting in the production of additional calcium silicate hydrate (C-S-H), the primary hydration product that contributes to the enhancement of mechanical strength [7]. The mechanical characteristics of TSC have been the subject of extensive research [1,2,4]. A number of factors considerably affect the mechanical characteristics of TSC, including the w/c and s/c ratios of the cement and sand, as well as the parameters of the coarse aggregate. SCMs were suggested as a potential material for enhancing the performance and durability of TSC [7]. Evaluating the mechanical properties of TSC necessitates considerable time, financial resources, and extensive experimentation [8,9]. The computational discipline of machine learning (ML) has emerged in recent decades to predict a variety of properties, thereby avoiding the costly and time-consuming process of conducting experiments [10–13]. Given these complexities, there is a growing need for advanced computational techniques to facilitate the prediction and optimization of TSC properties. ML offers a powerful approach to predicting concrete properties with high accuracy while reducing reliance on extensive experimental work. ML-based models can analyze vast datasets, recognize patterns, and provide reliable estimations of mechanical properties such as tensile strength (T-S). However, despite the success of ML in conventional concrete studies, its application in TSC research remains underexplored.

The properties of concrete have been predicted using a variety of ML algorithms, including artificial neural networks (ANNs) [14–16], gradient boosting [17–19], extreme learning machines [20,21], support vector regression [22,23], random forest (RF) [24,25], decision trees (DT) [26,27], gene expression programming (GEP) [28,29], XGBoost [30,31], and adaptive boosting [16,32]. The recent developments in ML approaches have generated new opportunities for the precise prediction of T-S. T-S is important because it ensures structural integrity and durability in applications subject to stretching or pulling forces [11,33]. For instance, an optimized support vector machine (SVM) model has been successfully implemented to estimate the splitting T-S at the bonding interface, achieving an error margin of less than 5% between the predicted and actual values [34]. Gradient boosting machine models were used to illustrate additional advancements in predictive modeling. These models demonstrated superior performance in estimating concrete T-S when compared to SVM [35]. ANNs have also demonstrated substantial potential as they circumvent conventional mathematical equations and rapidly adjust to new data, thereby expanding their applicability [36]. The accuracy of predictions and the number of errors have been significantly enhanced and reduced by ensemble learning techniques, such as bagging and boosting when applied to 1,030 datasets [16]. The optimization of predictive models remains a persistent challenge, particularly in the determination of the initial parameter values, despite these advancements [37]. Optimization techniques are employed to overcome these obstacles and improve the efficacy of the model [38,39]. These techniques enhance the model's performance by fine-tuning the relevant parameters, ensuring better accuracy and generalization [40–43]. These methods are essential for improving the accuracy of models and circumventing the constraints of traditional methods. Table 1 provides the details of the ML techniques employed in previous research studies.

Experimental testing is a resource-intensive and time-consuming procedure that necessitates specialized laboratory apparatus, an experienced workforce, and competent labor to guarantee the quality of TSC. Furthermore, the ecosystems in which they are introduced are adversely affected by sand, additives, and cement. Another environmental concern is the persistence of TSC specimens following the completion of testing. Consequently, the utilization of TSC in structures may prove to be affordable for the endeavor as a whole and more straightforward for the engineers involved if the necessary number of experimental experiments can be reduced. The objective of this investigation is to create a surrogate prediction model that employs ML algorithms to predict the T-S of TSC. This will result in a decrease in the number of environmental issues that must be addressed, as well as time and financial savings. Modeling material behavior is essential because it provides detailed insights into how materials will perform under various conditions, enabling better design and application strategies. GEP and RF are two powerful ML algorithms known for their effectiveness in predictive

Table 1: Previous researchers employed ML methodologies [44]

S. no	Applied ML methods	Predicted properties	Materials used	Total data points	Publication year	Ref.
1	MV	CS	Crumb rubber with SF	21	2020	[45]
2	RKSA	Slump, CS	FA	40	2018	[46]
3	GEP	CS	NZ (natural zeolite)	54	2019	[47]
4	ANFIS	CS	—	55	2018	[48]
5	GEP, MLR, and MNLR	CS	Bagasse ash	65	2020	[49]
6	ANN	CS	FA	69	2017	[50]
7	RSM, GEP	CS	Steel fibers	108	2020	[51]
8	IREMSVM-FR with RSM	CS	FA	114	2019	[52]
9	ANN	CS	FA	114	2017	[53]
10	M5MARS	CS, Slump	FA	114	2018	[26]
11	DEA	CS, Slump	FA	114	2021	[54]
12	SVM	Slump, CS	FA	115	2020	[55]
13	RF	CS	FA, GGBS	131	2019	[56]
14	ANN, DT, RF	T-S	Recycled aggregates	166	2022	[57]

modeling [58,59]. Consequently, GEP was employed to develop a T-S equation, and RF was incorporated as a result of its precise predictions and modeling capabilities. Ferreira proposed the concept of GEP in 2001 as an enhanced variant of genetic programming (GP) [60]. It employs a parse tree with branches of varying lengths and a string that is formatted in a straight line. The RF approach, also known as RF, was introduced in 2001 and is now considered an enhanced classification regression technique [61]. Consequently, the objective of this study is to establish a precise approach for predicting the T-S of TSC through the application of ML techniques. Two distinct methodologies were implemented to optimize the forecast's efficacy. This study is crucial as it addresses the challenge of accurately predicting TSC's T-S, a key property influencing its performance in construction applications.

Although ML-based predictions for TSC properties have been conducted in the past [62–64], no equation has been developed for predicting T-S. The experimental evaluation of TSC's mechanical properties remains time-consuming and costly, limiting large-scale research and practical implementation. Additionally, conventional methods for predicting TSC performance often lack accuracy and adaptability, while the influence of diverse input parameters on TSC properties remains underexplored in ML applications. To address these gaps, this study aims to develop a predictive equation for T-S using GEP and enhance modeling accuracy through RF. By leveraging advanced ML techniques, this research seeks to improve the precision of TSC predictions, optimize material performance through data-driven insights, and reduce reliance on extensive experimental work. Sensitivity analysis and SHapley Additive ExPlanation (SHAP) analysis were conducted to elucidate the link between the inputs and the outcome. The analysis sought to determine the most significant input factors that affect the target variable. The findings are anticipated to advance sustainable construction practices and facilitate better-informed decisions by contributing valuable knowledge to materials science and construction engineering.

2 Research methodology

The T-S of TSC is predicted in this investigation using GEP and RF. The research employs a structured methodology that commences with data acquisition and is subsequently followed by preprocessing to guarantee the quality of the data. Subsequently, the T-S is predicted using GEP and RF models in accordance with the input variables. Standard metrics are implemented to assess the models' functionality. Figure 1 illustrates the flowchart of the research methodology, which delineates the primary stages in the model development and validation process.

2.1 GEP

GEP has the ability to generate explicit mathematical equations, making it highly interpretable compared to black-box ML models. It effectively captures nonlinear relationships in complex datasets while offering robust generalization. Additionally, GEP's evolutionary approach optimizes model performance without overfitting, making it well-suited for predicting TSC properties. Ferreira was the pioneer in introducing GEP, a novel computational technique that serves as a subset of GP [60]. Experiments have demonstrated that GEP converges more quickly than traditional genetic algorithms [60]. Also, because the

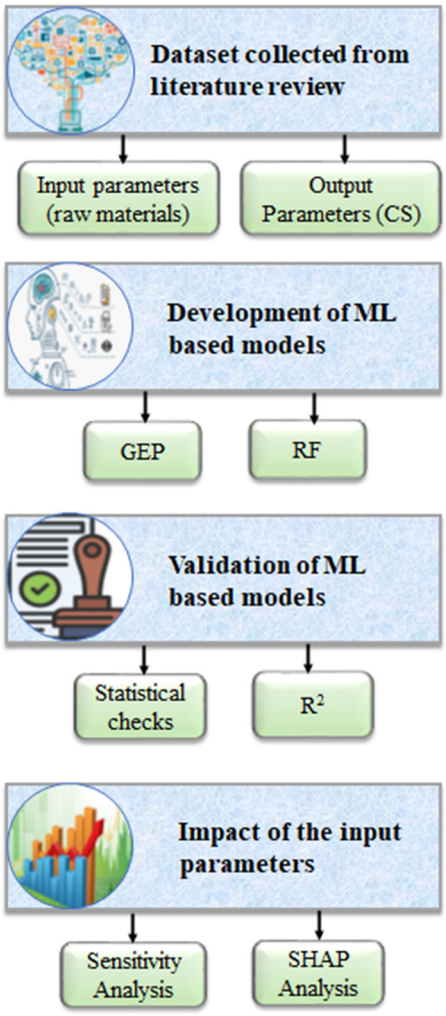

Figure 1: Flowchart of the study.

genetic manipulations are performed at the chromosomal level, there is more openness about the process [65]. Figure 2 is a simplified diagram of the primary GEP procedures. The procedure kicks off with the chromosomes of the founding population being generated at random. Then, the performance of each individual is measured against a collection of fitness instances based on the expression of these chromosomes. The individuals are then filtered based on their fitness (how well they do in that environment) to reproduce with alteration, producing offspring with novel characteristics. The same developmental process – genome expression, environmental conflict, selection, and modified reproduction – is then applied to these newly formed individuals. The procedure is continued until a satisfactory answer is discovered [66], which may take several generations.

In GEP, individuals are initially represented as linear strings of fixed-length (genomes). These genomes are then translated into complex structures of varying sizes and forms. Expression trees (ETs) identify these entities [67,68]. The typical human being consists of a single chromosome, each copy of which might contain anywhere from one to many genes. To produce offspring, a chromosome's expression, or ET, is subjected to a selection mechanism (often fitness proportional) based on the ET's fitness. The genetic operators do not alter the respective ET but rather the chromosomes during reproduction [47]. Open reading frames (ORFs) provide a better framework for understanding the structural organization of GEP genes. A gene's ORF consists of a "start" codon, the amino acid codons themselves, and a termination codon [60]. The genes speak one language, and ETs speak another in GEP.

In GEP, the phenotype can be directly derived from the genetic code, owing to the fundamental principles that govern the formation and functioning of ETs. Karva language is the name given to this mutually understandable bilingual notation [60,66]. Genetic operators make changes to the chromosomes during reproduction. Genetic operators in the GEP system include various processes such as duplication, alteration, rearrangement of genetic material, root and insertion sequence transpositions, recombination through single or double crossover, and gene transposition [60]. Each genetic operator in the GEP system has extensive documentation outlining its capabilities, which can be found in previous literature [65,69,70].

2.2 RF

The performance of individual trees within a forest can be predicted using a method called RF. This approach relies on values from a randomly generated vector, collected without bias, and applies a uniform distribution applied uniformly to all trees in the forest. As the quantity of trees in a forest significantly grows, the generalization error will eventually approach a limit. A forest of tree classifiers will have a generalization error that is proportional to the effectiveness of each tree in the forest and the interactions between the trees [56]. When a subset of features is chosen randomly to divide each node, the error rates are equal to those of AdaBoost; however, they are more resilient in terms of noise. Improvements in error, robustness, and connection measurement are achieved by internal assessments in reaction to increasing the amount of characteristics utilized for partitioning. This is done as a result of the increased number of features. Estimations made internally can also be utilized in the process of determining whether or not a variable is significant. These concepts are also

Figure 2: The stepwise procedure of the GEP technique [71].

relevant when thinking about regression. RFs are an effective method for making predictions [72]. They are able to avoid becoming too snug because of the law of huge numbers. They become reliable classifiers and regressors when the appropriate form of randomness is introduced into the process. Additionally, the framework gives insight into the forecasting capabilities of the RF with regard to the interactions between individual predictors and their efficacy. Instead, theoretical parameters like strength and correlation are estimated using out-of-bag data, and the results are more tangible [61]. Figure 3 shows the diagrammatic representation of the RF method.

2.3 Data collection

The information used to compile the TSC database could be found in a variety of published sources [3,6,8,74–84]. These sources were consulted in order to collect the necessary information. The frequency distribution of the database, which contains a total of 226 data points for tensile testing, is illustrated in Figure 4. The data was divided into two parts: 30% for assessment and 70% for training. Data preprocessing is the crucial stage of ML techniques. Preprocessing of data involves scanning it for any error or invalid entity. The current study was preprocessed using various statistical checks. Table 2 and Figure 5 provide information on the various statistical measures, including the highest and lowest possible values for each parameter and correlation coefficients. Table 2 also describes the standard deviation, median, mean, and sum of all the target and input regressors. These parameters provide a comprehensive overview of the data distribution, including the total, range, and central tendency. The minimum and maximum values indicate the spread of the data, while the mean and median offer insights into its average behavior and central position. The standard deviation highlights the variability, and the sum represents the cumulative value across all observations. It has been previously stated that the minimum ratio between the number of data points and input variables should be three. For a robust model, it is recommended that this ratio exceeds 5 [85]. In this case, the ratio is approximately 20.5, using 226 data points and 11 input factors, ensuring the adequacy of the dataset used for the ML modeling. Prior to the building of a model, the most important step that has an impact on the TSC's characteristics is input selection, and it takes place in this context. The running time of the developed models varies depending on their complexity and dataset size [86,87]. In order to produce a function that can be used in a more broad sense, the components of

concrete which have the most significant influence on the qualities of the concrete are extracted from the mixture. As part of this investigation, the TSC properties were looked at in relation to the following equation:

$$\text{TS} = f(\text{C, W, SF, SL, S, S/B, G, W/B, EA, FA, SP}). \quad (1)$$

A mix of domain knowledge and statistical methodologies were used to assess the TS of TSC. A detailed literature study and expert consultation resulted in the identification of a number of possible indicators, as shown in Eq. (1). These factors were chosen because they have been shown to influence the TS of TSC. A thorough feature importance analysis was conducted utilizing SHAP to evaluate the relative significance of the chosen indicators. This method facilitated a thorough evaluation of each feature's contribution to the model's predictions [30]. In addition to highlighting the most impactful input parameter, the SHAP analysis also helped identify potential multicollinearity issues, ensuring that the model remained robust and interpretable. As a result of this method, a more comprehensive knowledge of the underlying linkages among the attributes and the output parameter was made possible, which further enhanced the model's transparency and dependability. Moreover, as demonstrated by low pairwise correlations and consistent feature priority rankings across many model iterations, multicollinearity was not deemed to be a serious problem among the chosen features.

Data autoscaling and standardization are crucial for ML model performance because they mitigate the impact of features with greater values on model accuracy. After data normalization, the model is more accurate and stable since each variable is considered to have contributed equally. This process is essential for achieving results that are reliable and interpretable, particularly in the case of complex datasets. It was essential to normalize the original data before the ML algorithms began their analysis. The normalizing procedure not only improves computational stability but also reduces undesired feature scale effects [88]. Using Eq. (2), the range of values for each parameter was set to be between 0 and 0.9

$$y' = 0.9 \times \frac{y - y_{\min}}{y_{\max} - y_{\min}}, \quad (2)$$

where y is the initial value, $y_{\min}$ is the lowest value of the function, $y_{\max}$ is the highest value of the function, and y' is the normalized value.

2.4 Hyperparameter tuning of the models

Defining appropriate hyperparameters is essential for developing generalized and robust GEP and RF models. Hyperparameter optimization is achieved through systematic tuning techniques that combine trial and error with guidance from prior studies

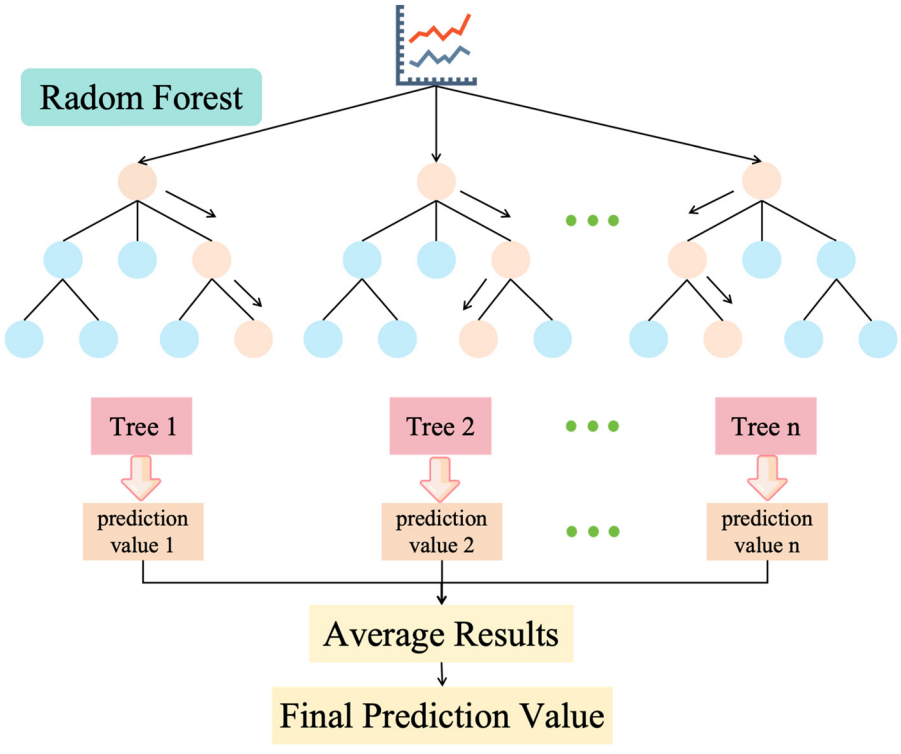

Figure 3: A diagrammatic representation of the RF method [73].

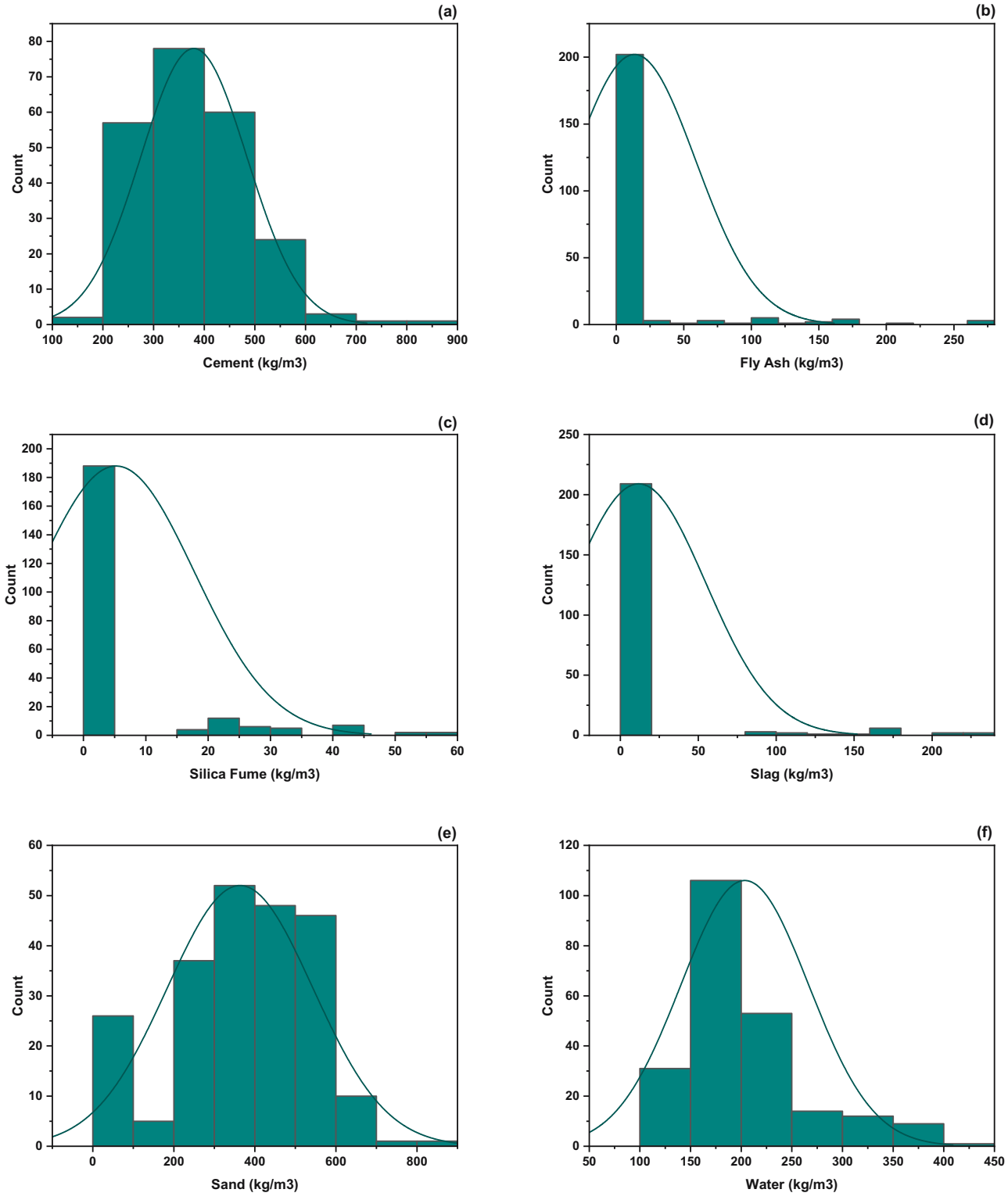

Figure 4: Frequency distribution: (a) cement, (b) fly ash, (c) SF, (d) slag, (e) sand, (f) water, (g) gravel, (h) W/B, (i) S/B, (j) superplasticizer, (k) expanding admixture, and (l) tensile strength.

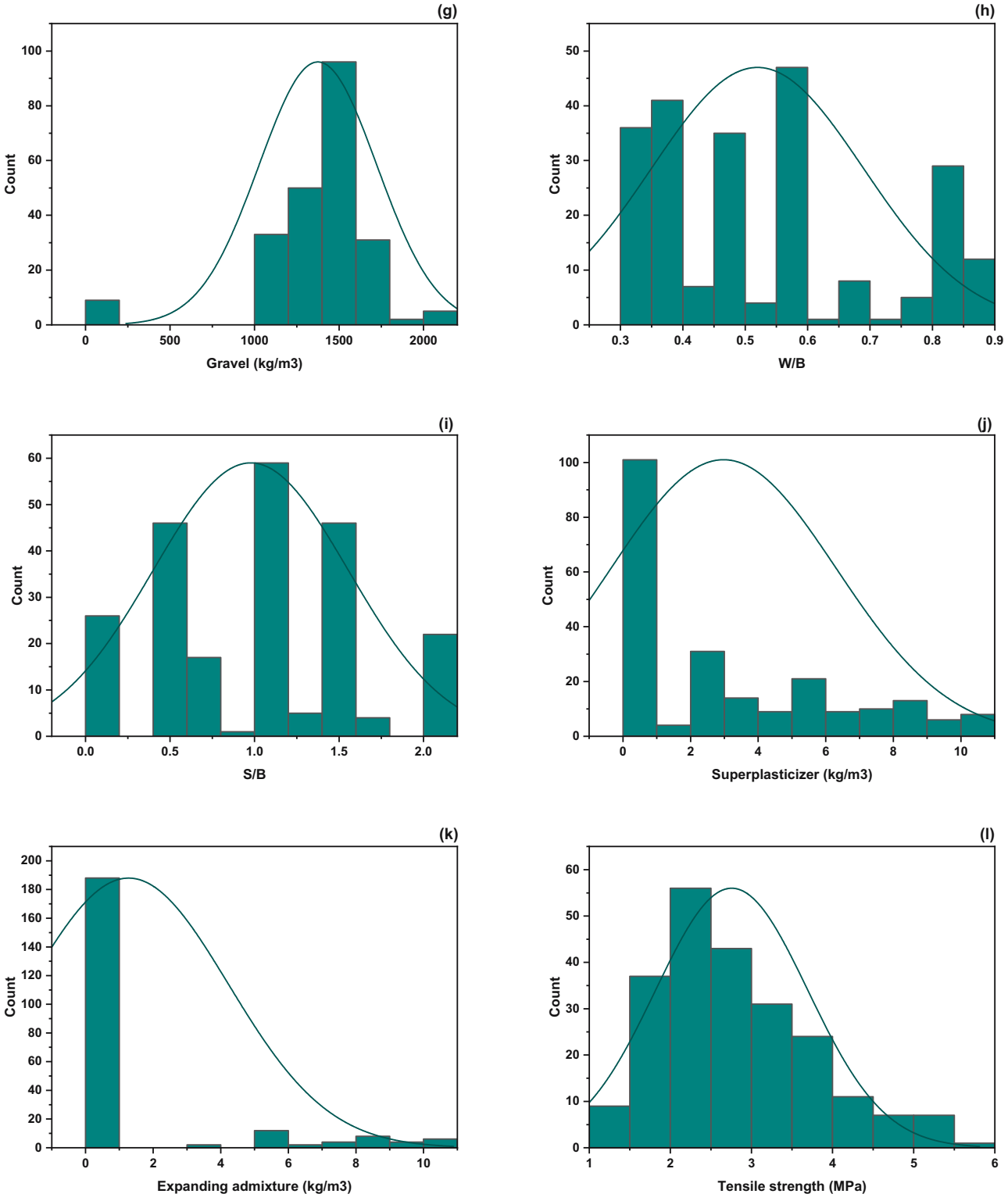

Figure 4: (*Continued*)

Table 2: Description of the parameters involved for TSC (inputs similar to [64])

Parameters	Units	Symbol	Total	Minimum	Maximum	Mean	Median	Standard deviation	Sum
Input									
Cement	(kg·m^{-3})	C	226	176.00	873.00	379.44	376.74	105.00	85754.02
Water	(kg·m^{-3})	W	226	100.00	431.00	203.54	191.85	63.14	46000.78
Slag	(kg·m^{-3})	SL	226	0.00	228.00	11.69	0.00	43.08	2643.00
W/B	—	W/B	226	0.30	0.85	0.52	0.47	0.17	117.44
SF	(kg·m^{-3})	SF	226	0.00	57.00	5.23	0.00	12.57	1183.02
S/B	—	S/B	226	0.00	2.00	0.98	1.00	0.58	220.91
Sand	(kg·m^{-3})	S	226	0.00	873.00	363.40	396.00	179.81	82129.26
Expanding admixture	(kg·m^{-3})	EA	226	0.00	10.50	1.27	0.00	2.95	287.86
Gravel	(kg·m^{-3})	G	226	1.56	2001.00	1375.06	1474.00	349.12	310764.27
Fly ash	(kg·m^{-3})	FA	226	0.00	262.00	13.51	0.00	45.43	3052.40
Superplasticizer	(kg·m^{-3})	SP	226	0.000	10.500	2.977	2.115	3.336	672.770
Output									
Tensile strength	MPa	T-S	226	1.200	5.500	2.756	2.600	0.939	622.900

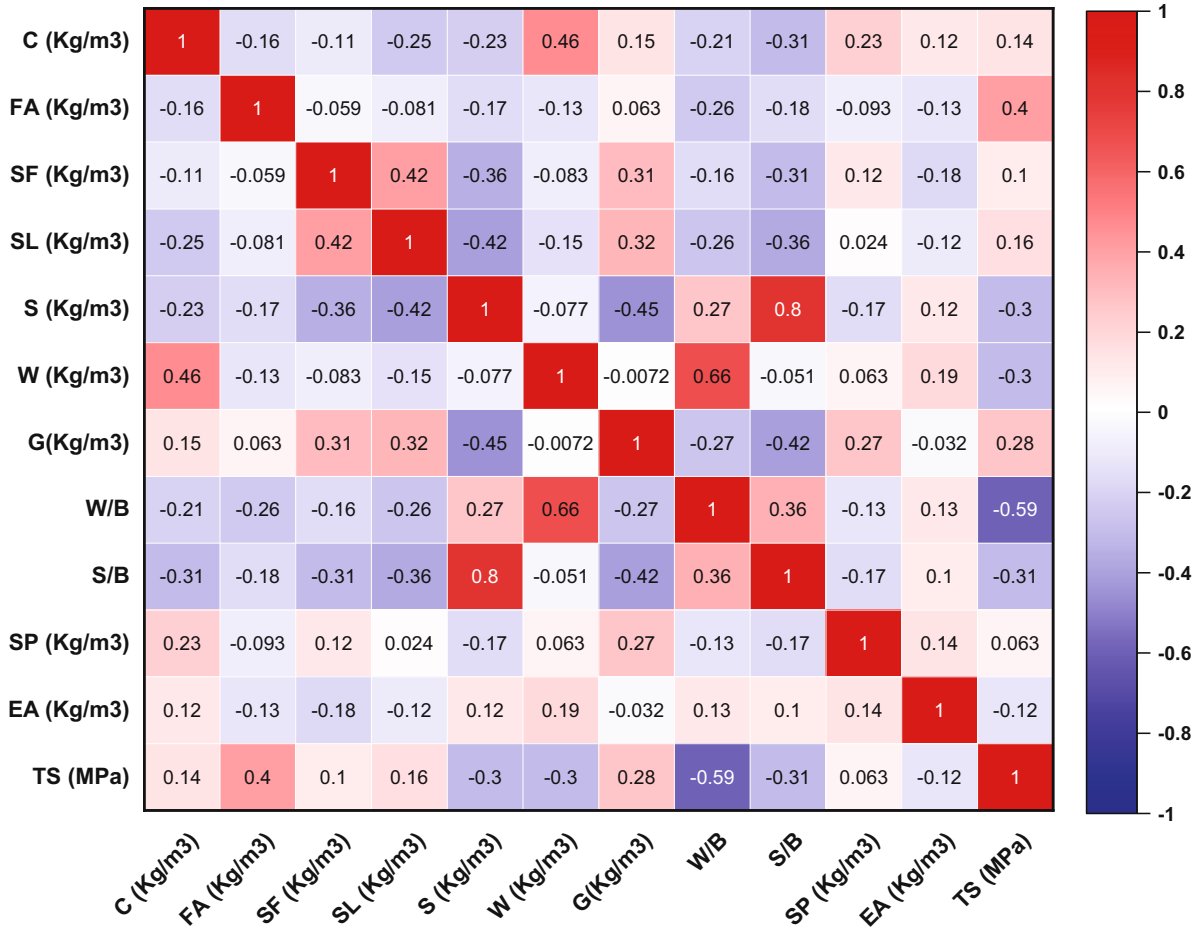

Figure 5: Pairwise correlation coefficient of T-S data.

[89], ensuring the models align effectively with the data. In the GEP model, hyperparameters such as population size, crossover rate, and mutation rate are adjusted to balance exploration and convergence, which enhances the model's ability to find optimal solutions while avoiding overfitting. As the population size increases, the model becomes more complex and accurate,

although it may take longer to align optimally with the data. Similarly, in the RF model, hyperparameters like the number of trees, maximum depth, and minimum samples split to control the model's complexity and generalization ability. Proper tuning of these parameters is crucial for optimizing model performance, ensuring it captures relevant patterns while maintaining a balance between accuracy and generalization. Table 3 outlines the hyperparameter ranges optimized for predicting TSC T-S.

2.5 Validation of models

The correctness of the model was determined for the dataset by examining its performance based on three metrics: the mean absolute error (MAE), mean squared error (MSE), the root mean squared error (RMSE), and the coefficient of determination (R^2). When estimating regression models for this kind of issue, these measures are utilized extensively [15,90,91]. Based on MAE and RMSE, the error criteria are employed to terminate the development of the models involved. To prevent overfitting, the models were suspended when these metrics reached predefined acceptable thresholds or demonstrated minimal improvement across iterations.

The MAE is a measurement that determines the mean size of the errors, which is the size of the disparity between the values that were seen and those that were anticipated [92]. Large mistakes brought about by outliers are almost never significant because the value being discussed is absolute and not quadratic [93]. Eq. (3) is used to calculate the MAE, which can range from zero to positive infinity, where P_i represents the actual value obtained from the experiment, M_i denotes the anticipated value, and n represents the overall count of occurrences. The model is considered to be of higher quality when its MAE is lower

$$\text{MAE} = \frac{1}{n}\sum_{i=1}^{n}|P_i - M_i|. \tag{3}$$

MSE is a widely utilized metric for evaluating the accuracy of regression models. It computes the average of the squared deviations between expected and observed values, as shown in Eq. (4). MSE is sensitive to outliers since it squares the data, giving greater mistakes a higher weight. A lower MSE suggests that the model is better fitted to the data. MSE is commonly used for model improvement and performance evaluation [43]

$$\text{MSE} = \frac{1}{n}\sum_{i=1}^{n}|P_i - M_i|^2. \tag{4}$$

The RMSE is a statistic that is frequently utilized for the purpose of measuring the extent of mistakes [92]. However, in contrast to the MAE, the RMSE tends to increase quite a bit when the error associated with each estimate grows due to the fact that it possesses a quadratic characteristic [93]. Eq. (5) is used to calculate RMSE. In the same vein as the MAE, having a low RMSE number is preferable

$$\text{RMSE} = \sqrt{\frac{\sum_{i=1}^{n}(P_i - M_i)^2}{N}}. \tag{5}$$

A statistic known as R^2 has values that can vary all the way from negative infinity to one [94]. As a result, R^2 will equal 1 if the model provides a perfect fit to the data, and the model will understand all of the data's variability [93]. Because the performance of the evaluated model is differentiated from that of a flat line, which is a reference model in which every forecast will correspond to the average of the outputs, the R^2 will be negative if the evaluated model offers a fit that is less satisfactory than that of the flat line of mean values. It is possible to calculate the R^2 by using Eq. (6), in which P_i represents the actual value received from the experiment, M_i represents the value anticipated by the model, and n represents the overall count of occurrences

$$R^2 = \frac{\sum_{i=1}^{n}(M_i - \bar{M}_i)(P_i - \bar{P}_i)}{\sqrt{\sum_{i=1}^{n}(M_i - \bar{M}_i)^2\sum_{i=1}^{n}(P_i - \bar{P}_i)^2}}. \tag{6}$$

Table 3: Configuration of hyperparameter values

Hyperparameter	GEP (range)	GEP (value)	RF (range)	RF (value)
Generations	50–400	200	—	—
Crossover rate	0.5–1.0	0.7	—	—
Population size	50–600	400	—	—
Tail length	5–50	20	—	—
Mutation rate	0.01–0.1	0.07	—	—
Head length	5–50	40	—	—
Maximum depth	—	—	5–50	30
Bootstrap samples	—	—	True/false	True
Number of trees	—	—	100–1,000	700
Minimum samples leaf	—	—	1–10	4
Random state	—	—	Integer or none	None
Minimum samples split	—	—	2–20	10

3 Results and discussion

3.1 Development of the GEP equation

In order to successfully evolve computer programs, genexpro tool software was used for GEP; the GEP method

makes use of a number of different factors. The length of the chromosome, which determines the size of the program representation, and the gene set, which includes all of the accessible functions and genes that are responsible for the construction of the programs, are the essential parameters. The length of the main program that is contained within the chromosome is characterized by the head length parameter, whereas the length of the remaining section is characterized by the tail length parameter. GEP is able to optimize its algorithmic behavior in order to provide the required outcomes in tasks such as symbolic regression, classification, and feature selection if these parameters are adjusted with care and attention. The configuration of the variables is specified in Table 4.

After configuring the GEP algorithm's settings in accordance with Table 4, as shown above, ETs, also known as ETs, are constructed by merging genes and functions from the gene set using the aforementioned criteria. The ETs are a representation of possible equations or solutions. The ETs are shown in Figure 6. They are assessed with fitness measurements that are unique to the issue and then optimized, utilizing those results. Techniques like genetic crossover, mutation, and selection are used during a series of iterative generations to bring about the evolution of the ETs. Eq. (7) displays the resulting equation that was obtained from the ET.

$$T - S = A + B + C + D, \tag{7}$$

where

$$A = \frac{\sqrt[3]{(S)} \times C + \mathrm{Ln}(W/B)}{9.61^2 - W}, \tag{7a}$$

$$B = \mathrm{Ln}((12.28 \times EA) + (SL + S) + EA^2 - (G \times \mathrm{Ln}(W/B))), \tag{7b}$$

$$C = \frac{1}{(8.92^2 + e^{SP}) + (2 \times SF) \times (FA - 0.32) - (FA - W/B)}, \tag{7c}$$

$$D = -4.53 - \frac{1}{(C + S/B) - (-2.47 - C) - (S + SL) + EA}, \tag{7d}$$

where T-S represents the tensile strength, S represents the sand, C represents the cement, W/B represents the water-to-binder ratio, W represents the water, EA represents the expanding admixture, SL represents the slag, G represents the gravel, SP represents the superplasticizer, FA represents the fly ash, S/B represents the superplasticizer-to-binder ratio, and SL represents the slag.

Table 4: Variables used to configure the GEP algorithm for implementation

Variables	Settings
Linking function	Addition
Chromosome	100
Function set	Ln, +, ×, ÷, −, $\sqrt[3]{}$. -
Head size	11
Genes	3
General	T-S

3.2 The outcome of the GEP model

The GEP method was employed to predict the T-S of TSC. The analysis revealed a coefficient of determination (R^2) of 0.91, indicating an excellent agreement between the predicted values and the experimentally observed results, as shown in Figure 7. The maximum prediction error recorded was 0.73 MPa, while the minimum error observed was 0.01 MPa, with an MAE of 0.19 MPa. An analysis of the error distribution demonstrated that 31.3% of the predictions had an error of 0.1 MPa or less, reflecting a high level of accuracy. Additionally, 62.6% of the predictions fell within an error range of 0.1–0.5 MPa, while only 6.1% exhibited errors exceeding 0.5 MPa. Figure 8 presents the distribution of errors for the experimental and predicted data. The close alignment between experimental and predicted values highlights the robustness of the GEP model in capturing the underlying relationship between input parameters and T-S. Furthermore, the low error margin reinforces the capability of GEP to approximate experimental outcomes with a high degree of precision. Collectively, these findings confirm that the GEP method is effective in predicting the T-S of TSC, supported by a high R^2 value and a low average prediction error.

3.3 The outcome of the RF model

The RF technique was also employed to predict the T-S of TSC. The analysis was conducted using Python programming, implemented *via* the Spyder (Anaconda software). The R^2 for the predictions was determined to be 0.94, indicating a strong correlation between the predicted values and the experimentally observed results, as shown in Figure 9. The maximum prediction error recorded was 0.55 MPa, while the minimum error observed was 0.02 MPa, with an MAE of 0.18 MPa. An analysis of the error

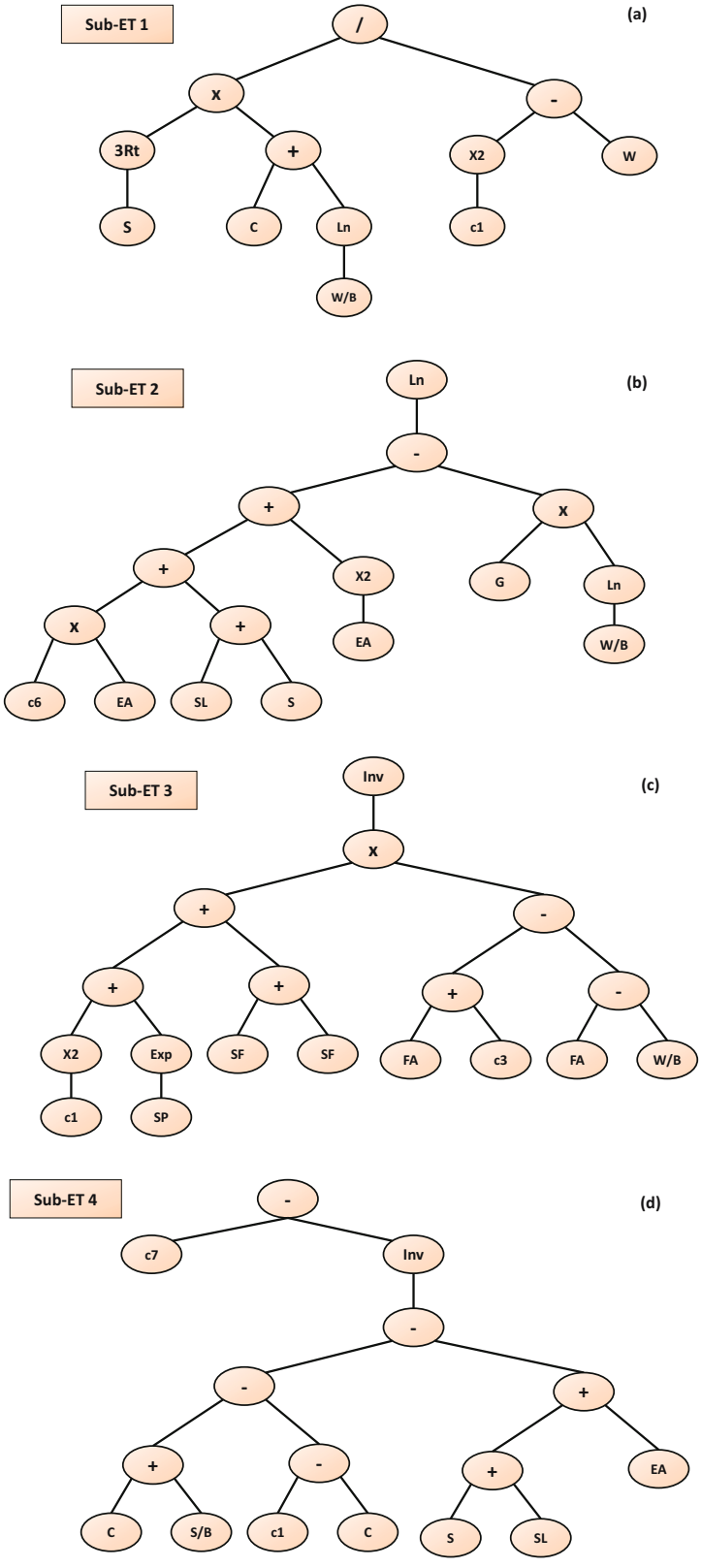

Figure 6: ET of TSC for T-S: (a) Sub-ET 1; (b) Sub-ET 2; (c) Sub-ET 3; and (d) Sub-ET 4.

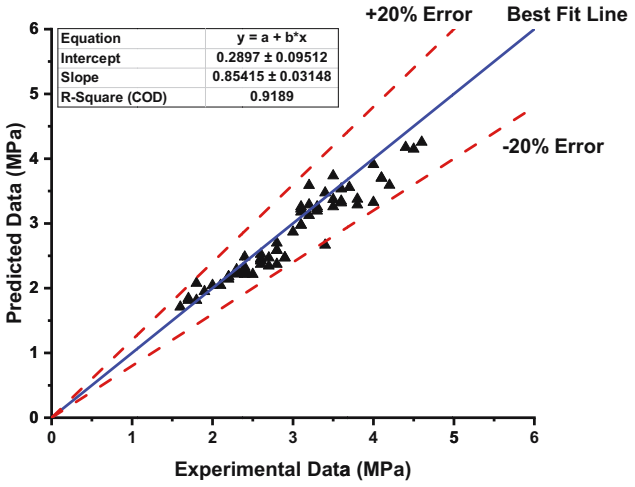

Figure 7: Performance evaluation of the experimental and predicted values for the GEP model.

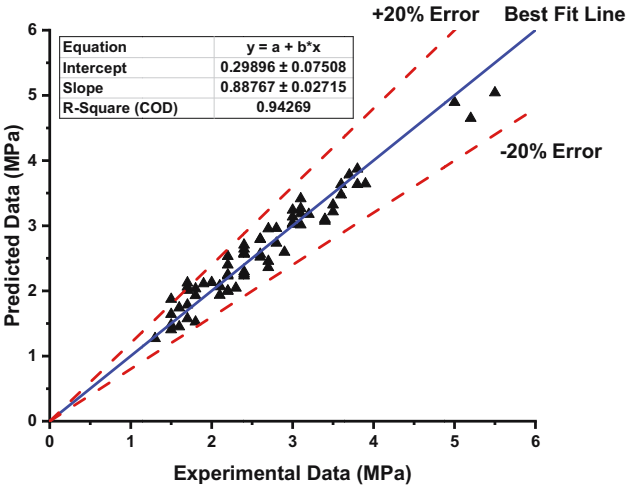

Figure 9: Performance evaluation of the experimental and predicted values for the RF model.

distribution revealed that 28.3% of the predictions had an error of 0.1 MPa or less, demonstrating a high degree of accuracy. Additionally, 70.1% of the predictions fell within an error range of 0.1–0.5 MPa, while only 1.6% exhibited errors exceeding 0.5 MPa. The alignment between the experimental and predicted values reinforces the reliability of the RF model in capturing the underlying relationships between input parameters and tensile strength. Figure 10 illustrates the distribution of errors for the experimental and predicted data.

The high R^2 value and the relatively low average prediction error affirm the effectiveness of the RF method in predicting the T-S of TSC. The RF model outperformed the GEP model in terms of predictive performance, as evidenced by a higher R^2 value. Furthermore, the concentration of predictions within acceptable error margins underscores the reliability of RF as a practical tool for forecasting the T-S of concrete. These findings imply that the RF model is better suited for practical applications where accurate and reliable predictions of T-S are crucial, particularly in TSC design and material optimization. This is primarily because the RF model can capture complex relationships between input parameters and T-S more effectively, making it a more reliable and accurate tool for predicting T-S in TSC.

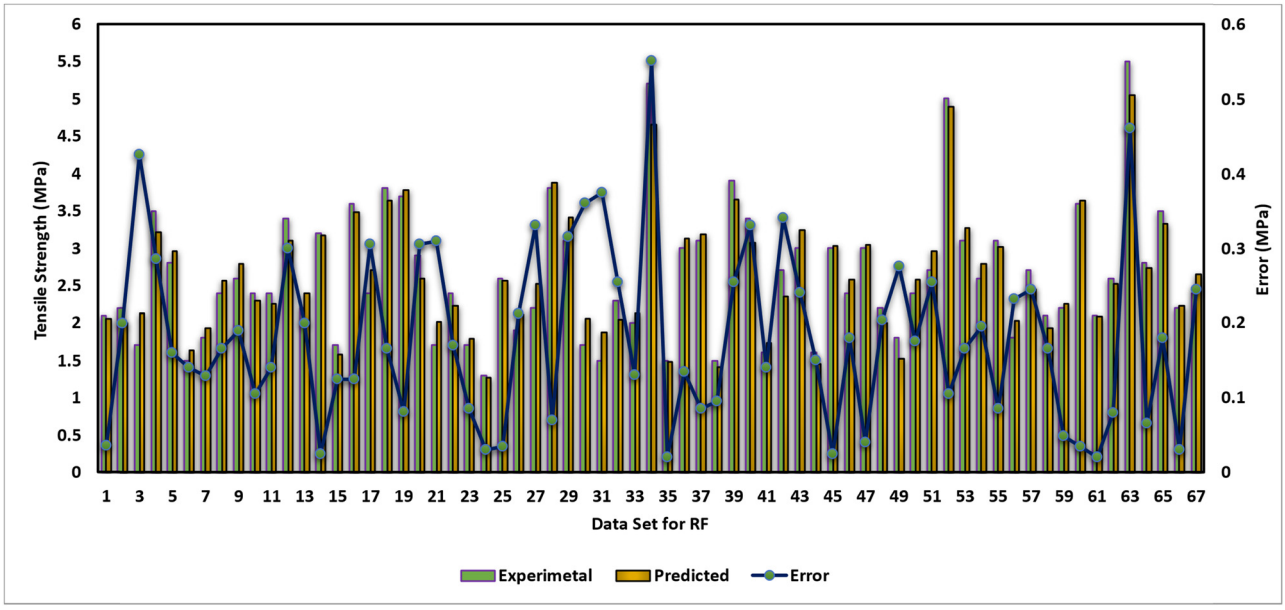

Figure 8: GEP model error distribution.

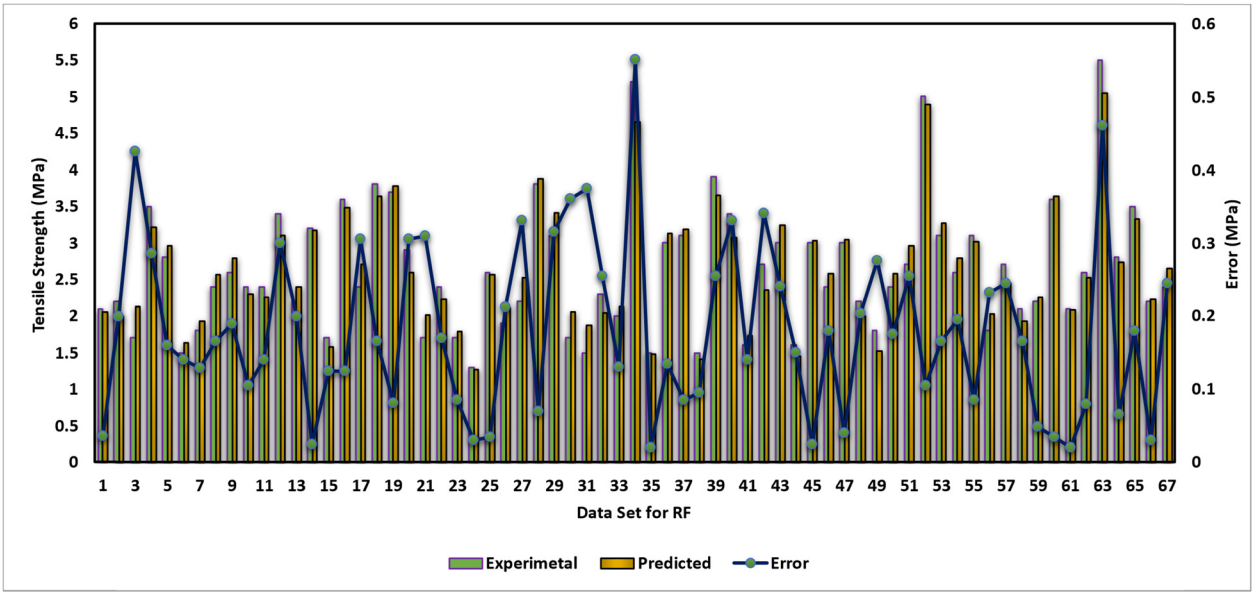

Figure 10: RF model error distribution.

3.4 Modeling based on statistical data evaluation

Presently, there are no models capable of accurately forecasting the T-S of TSC. Given the same range of input variables, Figure 11 demonstrates that RF models perform better than GEP models in predicting the T-S of TSC. The RF model, in contrast to other ML models, has the capability of effectively capturing the relationship between complex input factors and the output variables. When evaluated with the outcomes achieved by the GEP model, the MAE was determined to be 0.197 MPa, MSE was found to be 0.064 MPa, RMSE was found to be 0.254 MPa, and R^2 was found to be 0.91. Similarly, the RF model yielded MAE values of 0.181 MPa, MSE of 0.046 MPa, RMSE of 0.215 MPa, and R^2 of 0.94, respectively.

Following the completion of the investigation, the GEP model was developed. This model was subsequently used to generate predictions regarding the T-S of TSC and to assess the accuracy of those forecasts in comparison to those

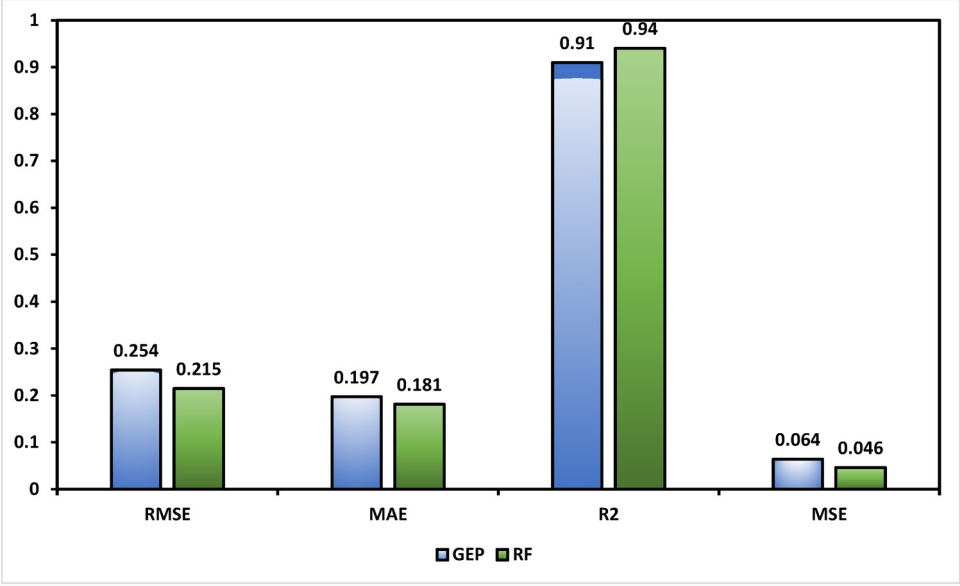

Figure 11: Statistical checks for the GEP and RF models.

generated by RF models. Given that the observed and anticipated values are more closely aligned, there is statistical evidence to imply that RF models are successful in forecasting the T-S of TSC. This proof comes in the form of statistics. The RF model demonstrates a minimum rate of error and higher R^2 values in comparison to the GEP ML approaches.

3.5 Sensitivity analysis

A model's expected output can be affected by changes to its input variables; therefore, conducting a sensitivity analysis is helpful. This method is crucial for assessing the stability and predictability of the model [95,96]. First, the problem has to be narrowed down by identifying the input factors that have an effect on the model's predicted value. After the variables were recognized, their respective intervals of variation were calculated. For the parameters under discussion, this range should contain values that are both acceptable and meaningful. By testing different values within the specified ranges, the relative importance and influence of each input variable on the model's output were determined using sensitivity analysis. This technique helps determine which factors have the most impact on forecasts and makes model-based decisions easier. A sensitivity assessment was performed to evaluate the effect of different factors on the T-S performance of TSC. The sensitivity analysis was conducted using the following equations:

$$N_i = f_{\max}(x_i) - f_{\min}(x_i), \tag{8}$$

$$\mathrm{SA} = \frac{N_i}{\sum_n^{j=1} N_j}. \tag{9}$$

The results illustrated the relative significance of the factors by displaying the percentage of the impact each input had on the output. It was revealed that the W/B had the greatest impact of around 51.01% among the components that were studied, which demonstrates the huge influence that it has on the T-S performance of the TSC. It was also observed in the previous investigation that the critical parameter for concrete strength is W/B [97]. Following that, gravel, water, and cement had the biggest influence on the T-S, contributing 23.52, 5.33, and 5.03%, respectively. The contributions of the remaining seven parameters on the T-S were less than 5%, as shown in Figure 12.

3.6 SHAP analysis results

The SHAP summary graphic illustrates the influence of various input characteristics on an ML model that forecasts T-S in TSC, as shown in Figure 13. The features, including the W/B, gravel, water, superplasticizer, cement, and other components, are ranked in order of their significance. The predicted T-S is considerably influenced by the most impactful feature, W/B, which is depicted at the top. Each dot on the figure represents the SHAP value for a single observation, indicating the degree to which each characteristic contributes to the T-S prediction. Positive SHAP values signify that a characteristic augments the T-S prediction, while negative ones attenuate it. The hue of the dots signifies the true value of the characteristic, with red dots representing high values and blue dots representing low values. The predicted T-S is increased by a high W/B ratio (represented by red dots), whereas lesser values (blue dots) have a reducing effect. The impacts of other

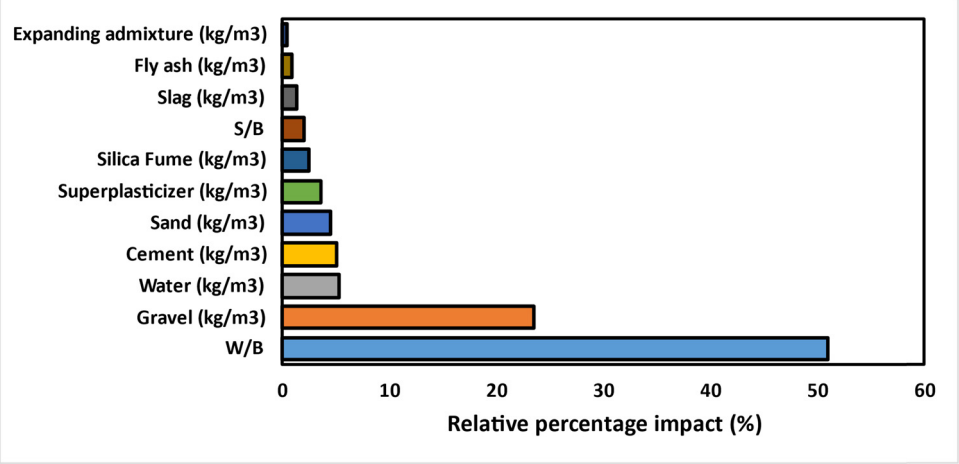

Figure 12: Sensitivity analysis of the TSC for the T-S.

features, such as water, superplasticizer, and gravel, are also variable. The horizontal spread of the dots for each feature indicates the extent of influence. Consistent effects are indicated by tightly concentrated dots, while a broader range of impacts is implied by more dispersed dots. These features importance provides essential insights for TSC design, as they highlight which material properties significantly influence T-S. For instance, the high impact of the W/B ratio suggests that adjusting this parameter can lead to better control over T-S, which is crucial for optimizing the mix design in TSC production. This plot provides valuable insights for optimizing T-S predictions by facilitating the interpretation of the contributions of individual material properties in the TSC mixture.

4 Discussion

TSC refers to the process of depositing coarse aggregate particles in an established formwork and subsequently occupying the gaps with a specialized cementitious mix. There are numerous differences between TSC and regular concrete. Initially, the components of traditional concrete are combined and thereafter placed in the formwork [63]. When making TSC, however, the grout components are mixed individually and then injected into the pre-arranged aggregate mass in the same way as previously explained. Not only that, but TSC has a greater percentage of coarse aggregate, which accounts for around 60% of the overall volume, whereas regular concrete normally accounts for approximately 40%. Through the placement of the aggregates in the formwork in advance, the TSC technique is able to assist in the resolution of the issue of coarse aggregate segregation, which is particularly prevalent in high-density aggregate concretes. In addition, TSC does not need to be consolidated, vibrated, or compressed in order to obtain a compact structure, which results in a reduction in the expenses associated with its manufacture [98]. As a result of these advantages, researchers are consistently investigating the mechanical characteristics of TSC.

The current trend in investigating the mechanical characteristics of TSC requires lab trials, which conversely influence the time and cost. However, in recent years, ML applications have been widely employed in the field of civil and material engineering to study the performance and characteristics of materials [99,100]. These ML techniques include SVM, DT, ANN, GEP, RF, bagging, and boosting [101–104]. Most of the studies in the past utilized ANN to predict the mechanical characteristics of concrete successfully. The current study is compared to the work of previous researchers who have implemented ML algorithms, as shown in Table 5. In addition, prior researchers have employed metrics such as R^2, MAE, and RMSE to assess the accuracy and performance of their models in predicting outputs [105]. In analytical studies, these statistical measures are frequently employed to evaluate the model's model fit and to quantify the discrepancies between predicted and actual values, thereby enabling a thorough comprehension of the model's predictive capabilities [105,106].

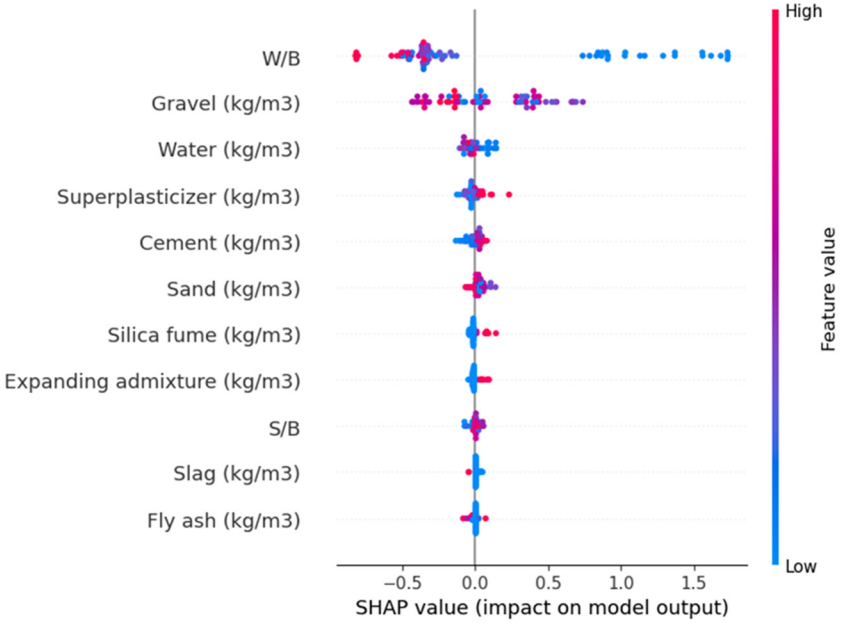

Figure 13: The influence of input parameters is illustrated in the SHAP plot.

Table 5: ML evaluation of the present study's findings in relation to pertinent previous studies

Ref.	Material studied	Property studied	Applied ML algorithms	Best-performing model
Present study	TSC	T-S	GEP and RF	RF
[64]	TSC	Compressive strength	GEP and RF	RF
[107]	Fly-ash based concrete	Compressive strength	GEP and RF	RF
[108]	High-strength concrete	Compressive strength	GEP and RF	RF
[109]	Concrete-filled steel tube columns	Bearing capacity of concrete	GEP, PSO, and ANN	GEP
[110]	Fly-ash based concrete	Compressive and T-S	GEP, MNLR, and RSM	GEP

However, to study the T-S of TSC, this study utilized GEP and RF techniques. GEP is an advanced technique utilized for symbolic regression and the creation of new features. It utilizes mathematical formulas to adapt computer programs to match the provided data. GEP provides the mathematical expression to compute the T-S of TSC, which can easily be computed and cross-checked by users. Similarly, RF is an effective ensemble learning method that builds many DTs and then combines their predictions. When training, each tree uses a different subset of the available data and parameters. By integrating the predictions of numerous trees, RF enhances the model's generalization performance and reduces overfitting. The results of this experiment show that the RF model performed better than the GEP model, as indicated by the RF model's greater values for R^2 and reduced MAE and RMSE results.

The RF and GEP models devised in this study offer advantages by operating within a predefined set of 11 independent variables (*i.e.*, cement, water, SF, slag, sand, S/B, gravel, W/B, expanding admixture, fly ash, and superplasticizer). This characteristic guarantees that the forecasts generated are tailored to the application of these materials in the context of predicting T-S. The model's adherence to a standardized testing procedure and the use of identical unit measurements establish the dependability of the T-S predictions they generate. The prescribed arithmetic equations of the ML models are of the utmost significance in understanding the ratio of the design of the mix and the impact on each variable that is independent. Nevertheless, the relevance of the ML forecasting algorithms may be compromised if additional variables are incorporated into the model equations in addition to the 11 variables previously mentioned [111]. It is possible that additional input variables will cause the produced models to fail because they were tailored to handle the particular collection of 11 input variables. The forecast models may also generate incorrect results if the input variable units are altered or if there are discrepancies. It is imperative that the units of the input parameter models match those employed in this study in order to guarantee that the models are deemed effective.

5 Conclusions and recommendations

The T-S characteristics of TSC are examined in this investigation using both GEP and RF ML algorithms. In order to enhance the predictive capabilities, both the GEP and RF strategies were implemented. Each input variable was meticulously analyzed to uncover its relative frequency distribution. In order to conduct RF analysis, the Spyder (Anaconda program) was modified using Python code, and the Genexpro tool was employed for GEP to conduct the requisite model simulations for further research. Multiple statistical tests were examined and evaluated to ensure the accuracy of the models being employed, including MAE, RMSE, and R^2. Furthermore, a sensitivity analysis was performed to investigate the potential impacts of all of the input variables. The subsequent findings were derived from the investigation's results.

- When it comes to predicting the T-S of TSC, the RF model provides a more accurate answer with less degree of variation.
- The value of the coefficient of correlation (R^2) for T-S according to the RF model is equal to 0.94, but the value of R^2 according to the GEP model is equal to 0.91.
- The excellent accuracy of the model is indicated by the relatively high values of R^2 for the RF regressor's contribution to the prediction of T-S.
- According to the statistical tests, the fact that the RF method has a lower value for errors (MAE and RMSE) shows that it has a higher level of performance when compared to the GEP algorithm.
- According to the results of the sensitivity analysis, the contribution of W/B to the prediction of the T-S of TSC was much higher than that of any other parameter, amounting to 51.01%.
- SHAP analysis also revealed that the W/B had the highest impact on T-S compared to all other components, followed by gravel. This insight can guide targeted adjustments to improve the T-S of TSC.

The study highlights that while the RF model outperforms GEP in predicting T-S of TSC, its effectiveness is limited by the dataset's scope and the use of only 11 input variables. Future research should focus on expanding the dataset and incorporating advanced ML techniques like gradient boosting, convolutional neural networks, and DTs. Exhaustive sensitivity analyses and exploring additional variables will improve predictive accuracy and understanding. The study emphasizes the importance of advanced ML in enhancing material performance for sustainable construction.

Acknowledgments: The authors acknowledge the Deanship of Scientific Research, Vice Presidency for Graduate Studies and Scientific Research, King Faisal University, Saudi Arabia (Grant No. KFU250709). The authors extend their appreciation for the financial support that made this study possible.

Funding information: This work was supported by the Deanship of Scientific Research, Vice Presidency for Graduate Studies and Scientific Research, King Faisal University, Saudi Arabia (Grant No. KFU250709).

Author contributions: M.N.A.: funding acquisition, supervision, project administration, investigation, writing, reviewing, and editing. F.J.: conceptualization, methodology, software, formal analysis, writing, reviewing, and editing. K.K.: visualization, resources, funding acquisition, formal analysis, writing, reviewing, and editing. S.A.K.: data acquisition, software, methodology, validation, writing-original draft. M.T.Q.: conceptualization, project administration, investigation, funding acquisition, writing, reviewing, and editing. M.K. investigation, resources, visualization, writing, reviewing, and editing. All authors have accepted responsibility for the entire content of this manuscript and approved its submission.

Conflict of interest: The authors state no conflict of interest.

Data availability statement: The datasets generated and/or analyzed during the current study are available as supplementary materials to this article.

References

[1] Abdelgader, H. S. Effect of the quantity of sand on the compressive strength of two-stage concrete. *Magazine of Concrete Research*, Vol. 48, 1996, pp. 353–360.

[2] O'Malley, J. and H. S. Abdelgader. Investigation into viability of using two-stage (pre-placed aggregate) concrete in Irish setting. *Frontiers of Architecture and Civil Engineering in China*, Vol. 4, 2010, pp. 127–132.

[3] Abdelgader, H. S. and J. Górski. Stress-strain relations and modulus of elasticity of two-stage concrete. *Journal of Materials in Civil Engineering*, Vol. 15, 2003, pp. 329–334.

[4] Bayer, R. İ. *Use of preplaced aggregate concrete for mass concrete applications*, Master's thesis, Middle East Technical University (Turkey), ProQuest, United States, 2004.

[5] Fang, B., Z. Qian, Y. Song, X. Diao, T. Shi, X. Cai, et al. Evaluation of early crack resistance performance of concrete mixed with ternary minerals using temperature stress testing machine (TSTM). *Journal of Cleaner Production*, Vol. 465, 2024, id. 142780.

[6] Abdelgader, H. S. How to design concrete produced by a two-stage concreting method. *Cement and Concrete Research*, Vol. 29, 1999, pp. 331–337.

[7] Aprianti, E. A huge number of artificial waste material can be supplementary cementitious material (SCM) for concrete production – a review part II. *Journal of Cleaner Production*, Vol. 142, 2017, pp. 4178–4194.

[8] Abdelgader, H. S., M. Kurpińska, and M. Amran. Effect of slag coal ash and foamed glass on the mechanical properties of two-stage concrete. *Materials Today: Proceedings*, Vol. 58, 2022, pp. 1091–1097.

[9] Chand, G., A. Kumar, and S. Ram. Comparative study of metakaolin, pumice powder and silica fume in producing treated sustainable recycled coarse aggregate concrete by adopting two-stage mixing. *Cleaner Engineering and Technology*, Vol. 9, 2022, id. 100528.

[10] Yu, Q., M. Monjezi, A. S. Mohammed, H. Dehghani, D. J. Armaghani, and D. V. Ulrikh. Optimized support vector machines combined with evolutionary random forest for prediction of back-break caused by blasting operation. *Sustainability*, Vol. 13, 2021, id. 12797.

[11] Lu, D., G. Wang, X. Du, and Y. Wang. A nonlinear dynamic uniaxial strength criterion that considers the ultimate dynamic strength of concrete. *International Journal of Impact Engineering*, Vol. 103, 2017, pp. 124–137.

[12] Song, X., W. Wang, Y. Deng, Y. Su, F. Jia, Q. Zaheer, et al. Data-driven modeling for residual velocity of projectile penetrating reinforced concrete slabs. *Engineering Structures*, Vol. 306, 2024, id. 117761.

[13] Fan, S., T. He, W. Li, C. Zeng, P. Chen, L. Chen, et al. Machine learning-based classification of quality grades for concrete vibration behaviour. *Automation in Construction*, Vol. 167, 2024, id. 105694.

[14] Chithra, S., S. R. R. S. Kumar, K. Chinnaraju, and F. Alfin Ashmita. A comparative study on the compressive strength prediction models for High Performance Concrete containing nano silica and copper slag using regression analysis and artificial neural networks. *Construction and Building Materials*, Vol. 114, 2016, pp. 528–535.

[15] Chou, J.-S., C.-F. Tsai, A.-D. Pham, and Y.-H. Lu. Machine learning in concrete strength simulations: Multi-nation data analytics. *Construction and Building Materials*, Vol. 73, 2014, pp. 771–780.

[16] Farooq, F., W. Ahmed, A. Akbar, F. Aslam, and R. Alyousef. Predictive modeling for sustainable high-performance concrete from industrial wastes: A comparison and optimization of models using ensemble learners. *Journal of Cleaner Production*, Vol. 292, 2021, id. 126032.

[17] Kazemi, F., N. Asgarkhani, and R. Jankowski. Machine learning-based seismic fragility and seismic vulnerability assessment of reinforced concrete structures. *Soil Dynamics and Earthquake Engineering*, Vol. 166, 2023, id. 107761.
[18] Ahmad, A., K. A. Ostrowski, M. Maślak, F. Farooq, I. Mehmood, and A. Nafees. Comparative study of supervised machine learning algorithms for predicting the compressive strength of concrete at high temperature. *Materials*, Vol. 14, 2021, id. 4222.
[19] Erdal, H. I. Two-level and hybrid ensembles of decision trees for high performance concrete compressive strength prediction. *Engineering Applications of Artificial Intelligence*, Vol. 26, 2013, pp. 1689–1697.
[20] Al-Shamiri, A. K., J. H. Kim, T.-F. Yuan, and Y. S. Yoon. Modeling the compressive strength of high-strength concrete: An extreme learning approach. *Construction and Building Materials*, Vol. 208, 2019, pp. 204–219.
[21] Han, B., Y. Wu, and L. Liu. Prediction and uncertainty quantification of compressive strength of high-strength concrete using optimized machine learning algorithms. *Structural Concrete*, Vol. 23, 2022, pp. 3772–3785.
[22] Golafshani, E. M. and A. Behnood. Application of soft computing methods for predicting the elastic modulus of recycled aggregate concrete. *Journal of Cleaner Production*, Vol. 176, 2018, pp. 1163–1176.
[23] Ribeiro, M. H. D. M. and L. dos Santos Coelho. Ensemble approach based on bagging, boosting and stacking for short-term prediction in agribusiness time series. *Applied Soft Computing*, Vol. 86, 2020, id. 105837.
[24] Dabiri, H., M. Kioumarsi, A. Kheyroddin, A. Kandiri, and F. Sartipi. Compressive strength of concrete with recycled aggregate; a machine learning-based evaluation. *Cleaner Materials*, Vol. 3, 2022, id. 100044.
[25] Iftikhar, B., S. C. Alih, M. Vafaei, M. A. Elkotb, M. Shutaywi, M. F. Javed, et al. Predictive modeling of compressive strength of sustainable rice husk ash concrete: Ensemble learner optimization and comparison. *Journal of Cleaner Production*, Vol. 348, 2022, id. 131285.
[26] Kaveh, A., T. Bakhshpoori, and S. M. Hamze-Ziabari. M5'and Mars based prediction models for properties of self-compacting concrete containing fly ash. *Periodica Polytechnica Civil Engineering*, Vol. 62, 2018, pp. 281–294.
[27] Alghamdi, S. J. Classifying high strength concrete mix design methods using decision trees. *Materials*, Vol. 15, 2022, id. 1950.
[28] Asif, U., S. A. Memon, M. F. Javed, and J. Kim. Predictive modeling and experimental validation for assessing the mechanical properties of cementitious composites made with silica fume and ground granulated blast furnace slag. *Buildings*, Vol. 14, 2024, id. 1091.
[29] Asif, U., M. F. Javed, M. Abuhussain, M. Ali, W. A. Khan, and A. Mohamed. Predicting the mechanical properties of plastic concrete: An optimization method by using genetic programming and ensemble learners. *Case Studies in Construction Materials*, Vol. 20, 2024, id. e03135.
[30] Utkarsh and P. K. Jain. Predicting bentonite swelling pressure: optimized XGBoost versus neural networks. *Scientific Reports*, Vol. 14, 2024, id. 17533.
[31] Argalis, P. P., M. Sinka, M. Andzs, A. Korjakins, and D. Bajare. Development of new bio-based building materials by utilising manufacturing waste. *Environmental and Climate Technologies*, Vol. 28, 2024, pp. 58–70.
[32] Nabipour, M., P. Nayyeri, H. Jabani, S. Shahab, and A. Mosavi. Predicting stock market trends using machine learning and deep learning algorithms via continuous and binary data; a comparative analysis. *IEEE Access*, Vol. 8, 2020, pp. 150199–150212.
[33] Sun, L., C. Wang, C. Zhang, Z. Yang, C. Li, and P. Qiao. Experimental investigation on the bond performance of sea sand coral concrete with FRP bar reinforcement for marine environments. *Advances in Structural Engineering*, Vol. 26, 2022, pp. 533–546.
[34] Jiang, W., Y. Xie, W. Li, J. Wu, and G. Long. Prediction of the splitting tensile strength of the bonding interface by combining the support vector machine with the particle swarm optimization algorithm. *Engineering Structures*, Vol. 230, 2021, id. 111696.
[35] Ray, S., M. M. Rahman, M. Haque, M. W. Hasan, and M. M. Alam. Performance evaluation of SVM and GBM in predicting compressive and splitting tensile strength of concrete prepared with ceramic waste and nylon fiber. *Journal of King Saud University - Engineering Sciences*, Vol. 35, 2023, pp. 92–100.
[36] Khan, M. I. Predicting properties of high performance concrete containing composite cementitious materials using artificial neural networks. *Automation in Construction*, Vol. 22, 2012, pp. 516–524.
[37] Shu, J., X. Zhang, W. Li, Z. Zeng, H. Zhang, and Y. Duan. Point cloud and machine learning-based automated recognition and measurement of corrugated pipes and rebars for large precast concrete beams. *Automation in Construction*, Vol. 165, 2024, id. 105493.
[38] Utkarsh, B. Ahmed, and P. K. Jain. Numerical analysis on structural behaviour of concrete-filled steel tubular columns. *In Proceedings of the Proceedings of the 2nd International Conference on Advances in Civil Infrastructure and Construction Materials (CICM 2023)*, Vol. 1, Cham, 2024, pp. 151–159.
[39] Yang, L. and A. Shami. On hyperparameter optimization of machine learning algorithms: Theory and practice. *Neurocomputing*, Vol. 415, 2020, pp. 295–316.
[40] Bui, D.-K., T. Nguyen, J.-S. Chou, H. Nguyen-Xuan, and T. D. Ngo. A modified firefly algorithm-artificial neural network expert system for predicting compressive and tensile strength of high-performance concrete. *Construction and Building Materials*, Vol. 180, 2018, pp. 320–333.
[41] Nguyen, M.-S. T., M.-C. Trinh, and S.-E. Kim. Uncertainty quantification of ultimate compressive strength of CCFST columns using hybrid machine learning model. *Engineering with Computers*, Vol. 38, 2022, pp. 2719–2738.
[42] Wu, Y. and S. Li. Damage degree evaluation of masonry using optimized SVM-based acoustic emission monitoring and rate process theory. *Measurement*, Vol. 190, 2022, id. 110729.
[43] Urkude, N., M. S. Hora, and Utkarsh. Enhancing machine learning models with metaheuristic Optimization techniques for accurate prediction of PSC in FRP-reinforced concrete slabs. *Mechanics of Advanced Materials and Structures*, 2024, pp. 1–17.
[44] Shang, M., H. Li, A. Ahmad, W. Ahmad, K. A. Ostrowski, F. Aslam, et al. Predicting the mechanical properties of RCA-based concrete using supervised machine learning algorithms. *Materials*, Vol. 15, 2022, id. 647. Doi: 10.3390/ma15020647.
[45] Shahmansouri, A. A., H. A. Bengar, and S. Ghanbari. Compressive strength prediction of eco-efficient GGBS-based geopolymer concrete using GEP method. *Journal of Building Engineering*, Vol. 31, 2020, id. 101326.
[46] Sathyan, D., K. B. Anand, A. J. Prakash, and B. Premjith. Modeling the fresh and hardened stage properties of self-compacting

concrete using random kitchen sink algorithm. *International Journal of Concrete Structures and Materials*, Vol. 12, 2018, id. 24.
[47] Shahmansouri, A. A., H. A. Bengar, and E. Jahani. Predicting compressive strength and electrical resistivity of eco-friendly concrete containing natural zeolite via GEP algorithm. *Construction and Building Materials*, Vol. 229, 2019, id. 116883.
[48] Vakhshouri, B. and S. Nejadi. Prediction of compressive strength of self-compacting concrete by ANFIS models. *Neurocomputing*, Vol. 280, 2018, pp. 13–22.
[49] Aslam, F., F. Farooq, M. N. Amin, K. Khan, A. Waheed, A. Akbar, et al. Applications of gene expression programming for estimating compressive strength of high-strength concrete. *Advances in Civil Engineering*, Vol. 2020, 2020, id. 8850535.
[50] Abu Yaman, M., M. Abd Elaty, and M. Taman. Predicting the ingredients of self compacting concrete using artificial neural network. *Alexandria Engineering Journal*, Vol. 56, 2017, pp. 523–532.
[51] Nematzadeh, M., A. A. Shahmansouri, and M. Fakoor. Post-fire compressive strength of recycled PET aggregate concrete reinforced with steel fibers: Optimization and prediction via RSM and GEP. *Construction and Building Materials*, Vol. 252, 2020, id. 119057.
[52] Selvaraj, S. and S. Sivaraman. Prediction model for optimized self-compacting concrete with fly ash using response surface method based on fuzzy classification. *Neural Computing and Applications*, Vol. 31, 2019, pp. 1365–1373.
[53] Belalia Douma, O., B. Boukhatem, M. Ghrici, and A. Tagnit-Hamou. Prediction of properties of self-compacting concrete containing fly ash using artificial neural network. *Neural Computing and Applications*, Vol. 28, 2017, pp. 707–718.
[54] Balf, F. R., H. M. Kordkheili, and A. M. Kordkheili. A new method for predicting the ingredients of self-compacting concrete (SCC) including fly ash (FA) using data envelopment analysis (DEA). *Arabian Journal for Science and Engineering*, Vol. 46, 2021, pp. 4439–4460.
[55] Saha, P., P. Debnath, and P. Thomas. Prediction of fresh and hardened properties of self-compacting concrete using support vector regression approach. *Neural Computing and Applications*, Vol. 32, 2020, pp. 7995–8010.
[56] Zhang, J., G. Ma, Y. Huang, J. sun, F. Aslani, and B. Nener. Modelling uniaxial compressive strength of lightweight self-compacting concrete using random forest regression. *Construction and Building Materials*, Vol. 210, 2019, pp. 713–719.
[57] Amin, M. N., A. Ahmad, K. Khan, W. Ahmad, S. Nazar, M. I. Faraz, et al. Split tensile strength prediction of recycled aggregate-based sustainable concrete using artificial intelligence methods. *Materials*, Vol. 15, 2022, id. 4296.
[58] Jiang, H., A. S. Mohammed, R. A. Kazeroon, and P. Sarir. Use of the gene-expression programming equation and FEM for the high-strength CFST columns. *Applied Sciences*, Vol. 11, 2021, id. 10468.
[59] He, B., S. H. Lai, A. S. Mohammed, M. M. Sabri, and D. V. Ulrikh. Estimation of blast-induced peak particle velocity through the improved weighted random forest technique. *Applied Sciences*, Vol. 12, 2022, id. 5019.
[60] Ferreira, C. Gene expression programming: a new adaptive algorithm for solving problems. *Complex Systems*, Vol. 13, No. 2, 2001, pp. 87–129.
[61] Breiman, L. Random forests. *Machine Learning*, Vol. 45, 2001, pp. 5–32.
[62] Moaf, F. O., F. Kazemi, H. S. Abdelgader, and M. Kurpińska. Machine learning-based prediction of preplaced aggregate concrete characteristics. *Engineering Applications of Artificial Intelligence*, Vol. 123, 2023, id. 106387.
[63] Rajabi, A. M., F. Omidi Moaf, and H. S. Abdelgader. Evaluation of mechanical properties of two-stage concrete and conventional concrete using nondestructive tests. *Journal of Materials in Civil Engineering*, Vol. 32, 2020, id. 04020185.
[64] Qureshi, H. J., M. Alyami, R. Nawaz, I. Y. Hakeem, F. Aslam, B. Iftikhar, et al. Prediction of compressive strength of two-stage (preplaced aggregate) concrete using gene expression programming and random forest. *Case Studies in Construction Materials*, Vol. 19, 2023, id. e02581.
[65] Wilson, S. W. Classifier conditions using gene expression programming. In *International workshop on learning classifier systems*, Springer Berlin Heidelberg, Berlin, Heidelberg, 2006, pp. 206–217.
[66] Ferreira, C. Gene expression programming in problem solving. In *Soft computing and industry: recent applications*, Roy, R., M. Köppen, S. Ovaska, T. Furuhashi, F. Hoffmann, eds., Springer London, London, 2002, pp. 635–653.
[67] Sarıdemir, M. Genetic programming approach for prediction of compressive strength of concretes containing rice husk ash. *Construction and Building Materials*, Vol. 24, 2010, pp. 1911–1919.
[68] Guven, A. and M. Gunal. Genetic programming approach for prediction of local scour downstream of hydraulic structures. *Journal of Irrigation and Drainage Engineering*, Vol. 134, 2008, pp. 241–249.
[69] Ferreira, C. *Gene expression programming: mathematical modeling by an artificial intelligence*, Vol. 21, Springer, New York, USA, 2006.
[70] Khawaja, L., M. F. Javed, U. Asif, L. Alkhattabi, B. Ahmed, and H. Alabduljabbar. Indirect estimation of resilient modulus (Mr) of subgrade soil: Gene expression programming vs multi expression programming. *Structures*, Vol. 66, 2024, id. 106837.
[71] Iftikhar, B., S. C. Alih, M. Vafaei, M. F. Javed, M. F. Rehman, S. S. Abdullaev, et al. Predicting compressive strength of eco-friendly plastic sand paver blocks using gene expression and artificial intelligence programming. *Scientific Reports*, Vol. 13, 2023, id. 12149.
[72] Han, Q., C. Gui, J. Xu, and G. Lacidogna. A generalized method to predict the compressive strength of high-performance concrete by improved random forest algorithm. *Construction and Building Materials*, Vol. 226, 2019, pp. 734–742.
[73] Li, X., K. Li, S. Shen, and Y. Tian. Exploring time series models for wind speed forecasting: a comparative analysis. *Energies*, Vol. 16, 2023, id. 7785.
[74] Tuyan, M., L. V. Zhang, and M. L. Nehdi. Development of sustainable preplaced aggregate concrete with alkali-activated slag grout. *Construction and Building Materials*, Vol. 263, 2020, id. 120227.
[75] Mohammadhosseini, H., M. M. Tahir, A. Alaskar, H. Alabduljabbar, and R. Alyousef. Enhancement of strength and transport properties of a novel preplaced aggregate fiber reinforced concrete by adding waste polypropylene carpet fibers. *Journal of Building Engineering*, Vol. 27, 2020, id. 101003.
[76] Lv, J., T. Zhou, and K. Li. Development and investigation of a new low-cement-consumption concrete – Preplaced aggregate concrete. *Sustainability*, Vol. 12, 2020, id. 1080.
[77] Das, K. K. *Development of high-performance preplaced aggregate concrete*, Pao Yue-kong Library, The Hong Kong Polytechnic University, Hung Hom, Kowloon, Hong Kong, 2022.
[78] Najjar, M. F., A. M. Soliman, and M. L. Nehdi. Critical overview of two-stage concrete: Properties and applications. *Construction and Building Materials*, Vol. 62, 2014, pp. 47–58.

[79] Coo, M. and T. Pheeraphan. Effect of sand, fly ash and limestone powder on preplaced aggregate concrete mechanical properties and reinforced beam shear capacity. *Construction and Building Materials*, Vol. 120, 2016, pp. 581–592.
[80] Coo, M. and T. Pheeraphan. Effect of sand, fly ash, and coarse aggregate gradation on preplaced aggregate concrete studied through factorial design. *Construction and Building Materials*, Vol. 93, 2015, pp. 812–821.
[81] Abdelgader, H. S. and A. A. Elgalhud. Effect of grout proportions on strength of two-stage concrete. *Structural Concrete*, Vol. 9, 2008, pp. 163–170.
[82] Prasad, N. and G. Murali. Exploring the impact performance of functionally-graded preplaced aggregate concrete incorporating steel and polypropylene fibres. *Journal of Building Engineering*, Vol. 35, 2021, id. 102077.
[83] Das, K. K. and S. S. E. Lam. Effect of coarse aggregate size and grouting process on properties of preplaced aggregate concrete. *Proceedings of the 4 World Congr on Civil, Structural, and Environmental Engineering (CSEE'19)*, 2019.
[84] Chairunnisa, N., H. Ruzhanah, and L. S. Daniel. The properties of preplaced aggregate concrete technology contain the industrial waste-material and the various shapes and sizes of coarse aggregate. *In IOP Conference Series: Materials Science and Engineering*, 2022, id. 012036.
[85] Gandomi, A. H. and D. A. Roke. Assessment of artificial neural network and genetic programming as predictive tools. *Advances in Engineering Software*, Vol. 88, 2015, pp. 63–72.
[86] He, L., B. Chen, Q. Liu, H. Chen, H. Li, W. T. Chow, et al. A quasi-exponential distribution of interfacial voids and its effect on the interlayer strength of 3D printed concrete. *Additive Manufacturing*, Vol. 89, 2024, id. 104296.
[87] Lu, D., F. Meng, X. Zhou, Y. Zhuo, Z. Gao, and X. Du. A dynamic elastoplastic model of concrete based on a modeling method with environmental factors as constitutive variables. *Journal of Engineering Mechanics*, Vol. 149, 2023, id. 04023102.
[88] Kumar, A., H. C. Arora, M. A. Mohammed, K. Kumar, and J. Nedoma. An optimized neuro-bee algorithm approach to predict the FRP-concrete bond strength of RC beams. *IEEE Access*, Vol. 10, 2021, pp. 3790–3806.
[89] Mousavi, S. M., A. H. Alavi, A. H. Gandomi, M. Arab Esmaeili, and M. Gandomi. A data mining approach to compressive strength of CFRP-confined concrete cylinders. *Structural Engineering & Mechanics*, Vol. 36, 2010, id. 759.
[90] Deepa, C., K. SathiyaKumari, and V. P. Sudha. Prediction of the compressive strength of high performance concrete mix using tree based modeling. *International Journal of Computer Applications*, Vol. 6, 2010, pp. 18–24.
[91] Bonifácio, A. L., J. C. Mendes, M. C. R. Farage, F. S. Barbosa, C. B. Barbosa, and A.-L. Beaucour. Application of support vector machine and finite element method to predict the mechanical properties of concrete. *Latin American Journal of Solids and Structures*, Vol. 16, 2019, id. e205.
[92] Willmott, C. J. and K. Matsuura. Advantages of the mean absolute error (MAE) over the root mean square error (RMSE) in assessing average model performance. *Climate Research*, Vol. 30, 2005, pp. 79–82.
[93] DeRousseau, M. A., E. Laftchiev, J. R. Kasprzyk, B. Rajagopalan, and W. V. Srubar. A comparison of machine learning methods for predicting the compressive strength of field-placed concrete. *Construction and Building Materials*, Vol. 228, 2019, id. 116661.
[94] Cameron, A. C. and F. A. G. Windmeijer. An R-squared measure of goodness of fit for some common nonlinear regression models. *Journal of Econometrics*, Vol. 77, 1997, pp. 329–342.
[95] Sin, G., K. V. Gernaey, and A. E. Lantz. Good modeling practice for PAT applications: propagation of input uncertainty and sensitivity analysis. *Biotechnology Progress*, Vol. 25, 2009, pp. 1043–1053.
[96] Asif, U., M. F. Javed, M. Alyami, and A. W. A. Hammad. Performance evaluation of concrete made with plastic waste using multi-expression programming. *Materials Today Communications*, Vol. 39, 2024, id. 108789.
[97] Yang, K.-H., A.-R. Cho, and J.-K. Song. Effect of water–binder ratio on the mechanical properties of calcium hydroxide-based alkali-activated slag concrete. *Construction and Building Materials*, Vol. 29, 2012, pp. 504–511.
[98] Najjar, M. F. *Innovating two-stage concrete with improved rheological, mechanical and durability properties*, The University of Western Ontario (Canada), ProQuest Dissertations & Theses, 2016, id. 29244255.
[99] Zhao, R., C. Li, and X. Guan. Advances in modeling surface chloride concentrations in concrete serving in the marine environment: A mini review. *Buildings*, Vol. 14, 2024, id. 1879.
[100] Guo, M., H. Huang, W. Zhang, C. Xue, and M. Huang. Assessment of RC frame capacity subjected to a loss of corner column. *Journal of Structural Engineering*, Vol. 148, 2022, id. 04022122.
[101] Güçlüer, K., A. Özbeyaz, S. Göymen, and O. Günaydın. A comparative investigation using machine learning methods for concrete compressive strength estimation. *Materials Today Communications*, Vol. 27, 2021, id. 102278.
[102] Yazdanpanah, O., K. M. Dolatshahi, and O. Moammer. Rapid seismic fragility curves assessment of eccentrically braced frames through an output-only nonmodel-based procedure and machine learning techniques. *Engineering Structures*, Vol. 278, 2023, id. 115290.
[103] Abdalla, A. and A. S. Mohammed. Hybrid MARS-, MEP-, and ANN-based prediction for modeling the compressive strength of cement mortar with various sand size and clay mineral metakaolin content. *Archives of Civil and Mechanical Engineering*, Vol. 22, 2022, id. 194.
[104] Yang, D., P. Xu, A. Zaman, T. Alomayri, M. Houda, A. Alaskar, et al. Compressive strength prediction of concrete blended with carbon nanotubes using gene expression programming and random forest: hyper-tuning and optimization. *Journal of Materials Research and Technology*, Vol. 24, 2023, pp. 7198–7218.
[105] Ali, R., M. Muayad, A. S. Mohammed, and P. G. Asteris. Analysis and prediction of the effect of Nanosilica on the compressive strength of concrete with different mix proportions and specimen sizes using various numerical approaches. *Structural Concrete*, Vol. 24, 2023, pp. 4161–4184.
[106] Alsharari, F., B. Iftikhar, M. A. Uddin, and A. F. Deifalla. Data-driven strategy for evaluating the response of eco-friendly concrete at elevated temperatures for fire resistance construction. *Results in Engineering*, Vol. 20, 2023, id. 101595.
[107] Khan, M. A., S. A. Memon, F. Farooq, M. F. Javed, F. Aslam, and R. Alyousef. Compressive strength of fly-ash-based geopolymer concrete by gene expression programming and random forest. *Advances in Civil Engineering*, Vol. 2021, 2021, pp. 1–17.
[108] Farooq, F., M. Nasir Amin, K. Khan, M. Rehan Sadiq, M. Faisal Javed, F. Aslam, et al. A comparative study of random forest and genetic engineering programming for the prediction of compressive strength of high strength concrete (HSC). *Applied Sciences*, Vol. 10, 2020, id. 7330.

[109] Sarir, P., J. Chen, P. G. Asteris, D. J. Armaghani, and M. M. Tahir. Developing GEP tree-based, neuro-swarm, and whale optimization models for evaluation of bearing capacity of concrete-filled steel tube columns. *Engineering with Computers*, Vol. 37, 2021, pp. 1–19.

[110] Shah, H. A., S. K. U. Rehman, M. F. Javed, and Y. Iftikhar. Prediction of compressive and splitting tensile strength of concrete with fly ash by using gene expression programming. *Structural Concrete*, Vol. 23, 2022, pp. 2435–2449.

[111] Chen, Z., B. Iftikhar, A. Ahmad, Y. Dodo, M. A. Abuhussain, F. Althoey, et al. Strength evaluation of eco-friendly waste-derived self-compacting concrete via interpretable genetic-based machine learning models. *Materials Today Communications*, Vol. 37, 2023, id. 107356.